VIP The following Communications have been judged by at least two referees to be “very important papers” and will be published online at www.angewandte.org soon:

C. Schäffer, A. Merca, H. Bögge, A. M. Todea, M. L. Kistler, T. Liu, R. Thouvenot, P. Gouzerh, A. Müller**
Unprecedented and Differently Applicable Pentagonal Units in a Dynamic Library: A Keplerate of the Type $\{(\mathrm{W})\mathrm{W}_5\}_{12}\{\mathrm{Mo}_2\}_{30}$

*S. W. Hong, M. Byun, Z. Lin**
Robust Self-Assembly of Highly Ordered Complex Structures by Controlled Evaporation of Confined Microfluids

L. Catala, D. Brinzei, Y. Prado, A. Gloter, O. Stéphan, G. Rogez, T. Mallah**
Core–Multishell Magnetic Coordination Nanoparticles: Towards Multifunctionality at the Nanoscale

*D. Morton, S. Leach, C. Cordier, S. Warriner, A. Nelson**
Synthesis of Natural-Product-Like Molecules with over Eighty Distinct Scaffolds

*P. Hazarika, S. M. Jickells, K. Wolff, D. A. Russell**
Imaging of Latent Fingerprints Through the Detection of Drugs and Metabolites

*O. Vendrell, F. Gatti, H.-D. Meyer**
Strong Isotope Effects in the Infrared Spectrum of the Zundel Cation

*W. M. Czaplik, M. Mayer, A. J. v. Wangelin**
Domino Iron Catalysis: Direct Aryl–Alkyl Cross-Coupling

Books

Spectroelectrochemistry	Wolfgang Kaim, Axel Klein	*reviewed by R. G. Compton*	**9378**
Iminosugars	Philippe Compain, Olivier R. Martin	*reviewed by K. Krämer*	**9378**

Correspondence

Polyoxometalates (1)

R. Cao, T. M. Anderson, D. A. Hillesheim, P. Kögerler, K. I. Hardcastle, C. L. Hill* ———— **9380–9382**

Platinum-Containing Polyoxometalates

Late-transition-metal terminal oxo compounds: criticisms, analysis, and responses concerning the Pt-containing polyoxovanadate $[\mathrm{H_2Pt^{IV}V_9O_{28}}]^{5-}$ reported by Lee, Kortz, and their co-workers are presented. It is also deduced that a terminal platinum oxo compound from one of their groups, reported elsewhere but cited in connection with $[\mathrm{H_2Pt^{IV}V_9O_{28}}]^{5-}$, is missassigned.

Polyoxometalates (2)

U. Kortz,* U. Lee,* H.-C. Joo, K.-M. Park, S. S. Mal, M. H. Dickman, G. B. Jameson ———— **9383–9384**

Platinum-Containing Polyoxometalates

The comments of Hill and co-workers regarding the platinum-containing polyoxovanadate $[\mathrm{H_2Pt^{IV}V_9O_{28}}]^{5-}$ are responded to by Kortz, Lee and co-workers. In addition, the existence of the anion $\alpha\text{-}[\mathrm{SiW_{10}Pt^{IV}{}_2O_{40}}]^{8-}$ and the platinum oxo complex $[\mathrm{O{=}Pt^{IV}(H_2O)(PW_9O_{34})_2}]^{16-}$ are discussed.

Contents

Highlights

Biosynthesis

B. S. Moore* ______________ **9386 – 9388**

Extending the Biosynthetic Repertoire in Ribosomal Peptide Assembly

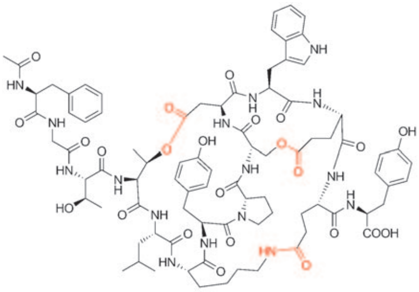

An extended family: The addition of microviridin B (see structure) and trunkamide to the ribosomal peptide biosynthetic family extends the molecular basis of posttranslational modifying reactions to include ω-ester/ω-amide linkage by ATP-grasp ligases (red) and prenylation. The discovery of these novel secondary metabolic reactions may presage the bioengineering of new antimicrobial peptide libraries.

Cortistatin A

C. F. Nising,* S. Bräse* ____ **9389 – 9391**

Highlights in Steroid Chemistry: Total Synthesis versus Semisynthesis

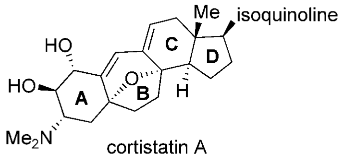

Many routes to the destination: Cortistatins are steroids of marine origin of which cortistatin A has the highest antiangiogenetic action. Several total syntheses of this natural product have recently been achieved, based on biosynthesis, biomimetic synthesis, semisynthesis, and de novo synthesis, which are compared in this Highlight.

Essays

History of Science

J. M. Thomas* ______________ **9392 – 9401**

Lord Rutherford (1871–1937): The Newton of the Atom and the Winner of the Nobel Prize for Chemistry, 1908

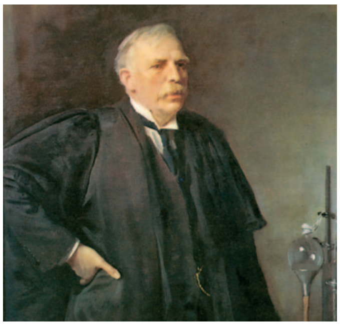

On the shoulders of giants: Lord Rutherford, who developed the theory of nuclear disintegration and a model of the nuclear atom, was lauded as one of the greatest scientists of all time. His research career witnessed the beginning of the atomic age, and his research group was a hotbed of talented, young scientists.

For the USA and Canada: ANGEWANDTE CHEMIE International Edition (ISSN 1433-7851) is published weekly by Wiley-VCH, PO Box 191161, 69451 Weinheim, Germany. Air freight and mailing in the USA by Publications Expediting Inc., 200 Meacham Ave., Elmont, NY 11003. Periodicals postage paid at Jamaica, NY 11431. US POSTMASTER: send address changes to *Angewandte Chemie*, Wiley-VCH, 111 River Street, Hoboken, NJ 07030. Annual subscription price for institutions: US$ 7225/6568 (valid for print and electronic / print or electronic delivery); for individuals who are personal members of a national chemical society prices are available on request. Postage and handling charges included. All prices are subject to local VAT/sales tax.

Reviews

Natural Product Synthesis

G. E. Veitch, A. Boyer,
S. V. Ley* ______ 9402 – 9429

The Azadirachtin Story

Long and winding road: The natural product azadirachtin (see figure) was first isolated in 1968 from the neem tree, and has been the focus of intense research efforts ever since. With numerous obstacles now overcome, the international efforts towards the total synthesis of this fascinating molecule have now achieved their long-standing goal.

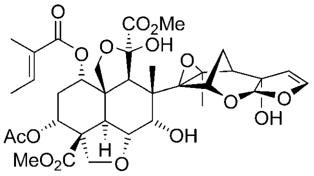

Communications

Hypervalent Compounds

N. Kano,* Y. Itoh, Y. Watanabe, S. Kusaka,
T. Kawashima* ______ 9430 – 9433

Structure and Properties of a Sulfur(IV)–Sulfur(II)-Bond Compound: Reversible Conversion of a Sulfur-Substituted Organosulfurane into a Thiol

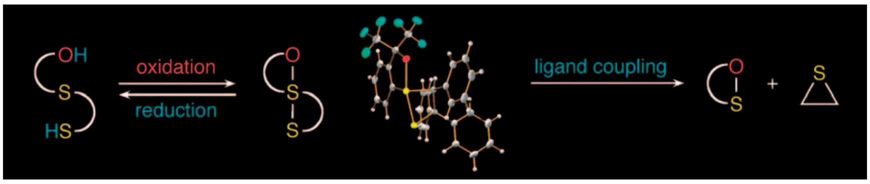

A highly polar hypervalent S^{IV}–S^{II} bond was formed in the synthesis of a sulfur-substituted sulfurane (see scheme), which was crystallographically characterized. Reduction of the 1,2-dithietane gives the corresponding thiol, and reoxidation gives the sulfurane by S–S bond formation. Thermal decomposition leads to a cyclic sulfenate and a thiirane.

Homogeneous Catalysis

J. Spielmann, F. Buch,
S. Harder* ______ 9434 – 9438

Early Main-Group Metal Catalysts for the Hydrogenation of Alkenes with H_2

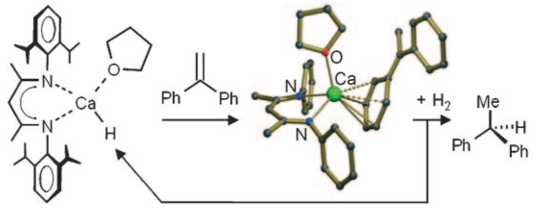

Transition-metal-free hydrogenation of alkenes can be carried out with simple organocalcium catalysts (20 bar H_2, 20 °C). Both steps in the proposed catalytic cycle, hydride addition to the double bond and σ-bond metathesis with H_2, have been confirmed. Alkenes sensitive to polymerization are also hydrogenated in good yields.

Synthetic Methods

T. Lanza, R. Leardini, M. Minozzi,*
D. Nanni,* P. Spagnolo,*
G. Zanardi ______ 9439 – 9442

Approach to Spirocyclohexadienimines and Corresponding Dienones through Radical *ipso* Cyclization onto Aromatic Azides

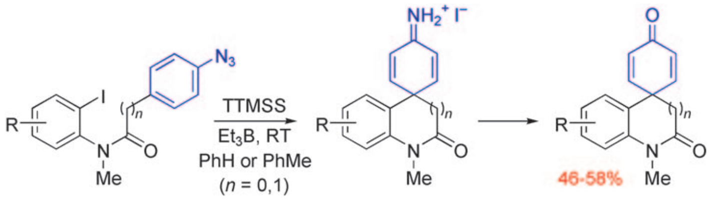

***Ipso* easy**: Cyclization of aryl radicals at the *ipso*-position of *p*-azido-substituted benzamides or 2-phenylacetamides results in effective production of spirocyclohexadieniminyl radicals through prompt elimination of molecular nitrogen by transient azidocyclohexadienyl radicals. The resultant iminyl radicals can be exploited for the synthesis of oxindoles or quinolones bearing spiro-cyclohexadienimine/cyclohexadienone rings (see picture, TTMSS = tris(trimethylsilyl)silane).


A Journal of the Gesellschaft Deutscher Chemiker
Angewandte Chemie
International Edition
GDCh
D 3461
www.angewandte.org
2008–47/16
WILEY-VCH

Radical Reactions

N. Charrier, S. Z. Zard* ____ **9443–9446**

Radical Allylation with α-Branched Allyl Sulfones

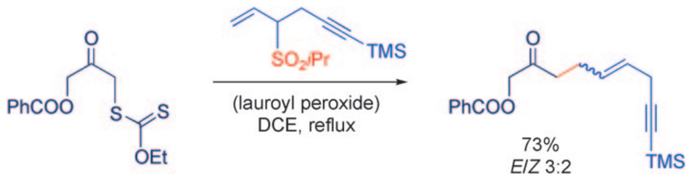

Branching out with sulfones: The use of allyl isopropyl sulfones solves the problem of premature isomerization and allows the radical addition of xanthates to α-branched allyl sulfones (see scheme; DCE = 1,2-dichloroethane, TMS = trimethylsilyl). Highly functionalized structures can thus be rapidly assembled under mild reaction conditions by using cheap and readily available substrates and reagents.

Carboranes

J. Zhang, H.-S. Chan, Z. Xie* ____ **9447–9449**

Reaction of 13-Vertex Carboranes with Nucleophiles: Unprecedented Cage-Carbon Extrusion and Formation of Monocarba-*closo*-dodecaborate Anions

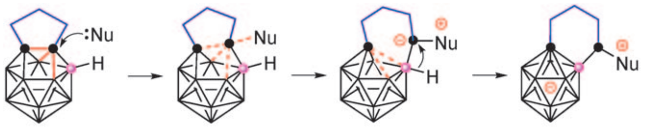

In contrast to icosahedral carboranes, instead of deboration, 13-vertex carboranes undergo cage-carbon extrusion and cluster contraction to give icosahedral monocarborane anions on reaction with nucleophiles. In the proposed mechanism, nucleophilic attack on a cage carbon atom cleaves the C_{cage}–C_{cage} bond, new C_{cage}–B bonds form to preserve cluster integrity, and hydrogen migration generates the final icosahedral product (see scheme).

Natural Products

N. A. McGrath, C. A. Lee, H. Araki, M. Brichacek, J. T. Njardarson* ____ **9450–9453**

An Efficient Substrate-Controlled Approach Towards Hypoestoxide, a Member of a Family of Diterpenoid Natural Products with an Inside-Out [9.3.1]Bicyclic Core

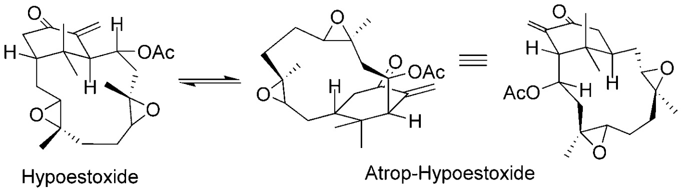

The bicycle works: A versatile route to the verticillane family of natural products has been devised, utilizing a strategically rigidified relay ring-closing metathesis reaction. The shape of the bicyclic product was used to stereoselectively control the bisepoxidation reaction towards hypoestoxide, a member of this natural product family.

Asymmetric Synthesis

T. Yue, M.-X. Wang,* D.-X. Wang, J. Zhu* ____ **9454–9457**

Asymmetric Synthesis of 5-(1-Hydroxyalkyl)tetrazoles by Catalytic Enantioselective Passerini-Type Reactions

Three-part harmony: Three-component Passerini reactions (P-3CR, see Scheme) of a wide range of aldehydes **2** and isocyanides **3**, with hydrazoic acid **4** in toluene, in the presence of a [(salen)AlMe]-complex catalyst afford 5-(1-hydroxyalkyl)tetrazoles **1** in good-to-excellent yields and enantiomeric excess. A tandem Michael addition/enantioselective P-3CR, using an acrolein substrate, affords highly functionalized tetrazoles.

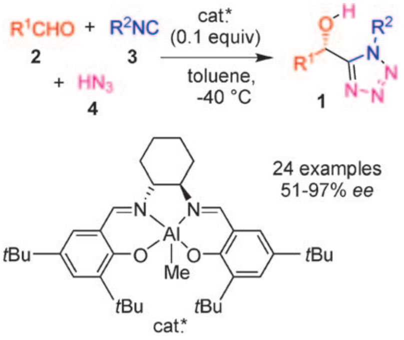

Contents

Asymmetric Catalysis

D. Minato, Y. Nagasue, Y. Demizu,
O. Onomura* ____________ **9458 – 9461**

Effecient Kinetic Resolution of Racemic Amino Aldehydes by Oxidation with *N*-Iodosuccinimide

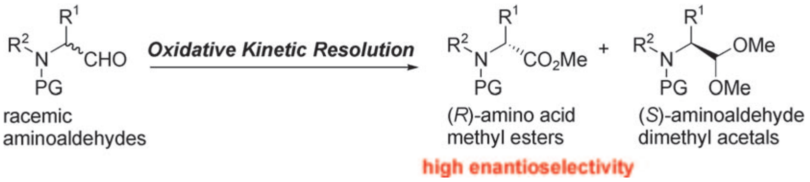

Selective recognition: The first efficient method for the kinetic resolution of racemic amino aldehydes (see scheme, PG = protecting group) is based on a copper(II)/(*R*,*R*)-Ph-BOX complex. The coordinated amino aldehydes were transformed into optically active amino acid methyl esters, and the non-coordinated amino aldehydes were converted into optically active amino aldehyde dimethyl acetals.

Synthetic Methods

V. S. Thirunavukkarasu, K. Parthasarathy,
C.-H. Cheng* ____________ **9462 – 9465**

Synthesis of Fluorenones from Aromatic Aldoxime Ethers and Aryl Halides by Palladium-Catalyzed Dual C—H Activation and Heck Cyclization

Highway to Heck: An efficient new one-pot palladium-catalyzed synthesis is described which affords a wide range of 9-fluorenone derivatives in good to excellent yields. A mechanism for the two distinct catalytic steps, C—H bond activation followed by oxidative intramolecular Heck cyclization, is proposed and reaction intermediates supporting this mechanism have been isolated.

Phase-Transfer Catalysis

R. He, X. Wang, T. Hashimoto,
K. Maruoka* ____________ **9466 – 9468**

Binaphthyl-Modified Quaternary Phosphonium Salts as Chiral Phase-Transfer Catalysts: Asymmetric Amination of β-Keto Esters

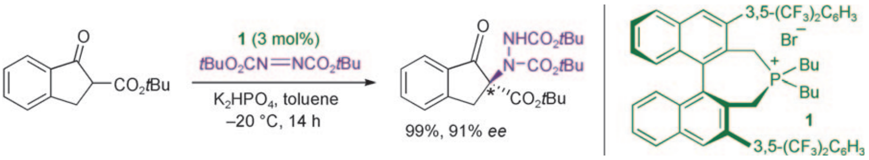

A reliable phosphonium-based PTC: For the first time a chiral quaternary tetraalkylphosphonium salt has successfully been used as a phase-transfer catalyst (PTC) for asymmetric amination of β-keto esters, in high yield and with high *ee* (see scheme). Asymmetric amination of a cyclic five-membered β-keto ester is a valuable method for preparing a key intermediate for asymmetric synthesis of aldose reductase inhibitor AS-3201 (Ranirestat).

Semiconductors

J. Zhang, P. Chen, G. Shen,
J. He, A. Kumbhar, C. Zhou,
J. Fang* ____________ **9469 – 9471**

p-Type Field-Effect Transistors of Single-Crystal Zinc Telluride Nanobelts

Is ZnTe it great: Controlling the crystal-growth direction leads to formation of single-crystal ZnTe nanobelts along the $\langle\bar{2}00\rangle$ direction. The nanobelts, which were synthesized in oleylamine at 250 °C, have a narrow thickness (< 6 nm). The ZnTe nanobelts behave as p-type semiconductors in field-effect transistors (see picture).

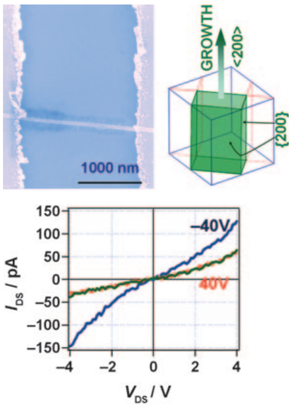

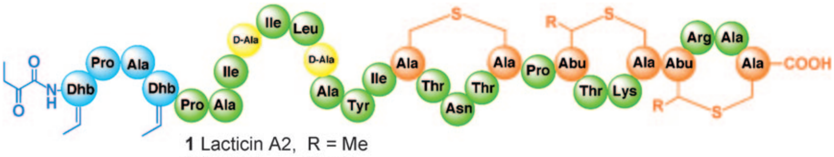

1 Lacticin A2, R = Me
2 Lan A2, R = H

Lan-tastic! A lanthionine analogue of lacticin 3147 A2 (Lan-A2, **2**) containing multiple thioether bridges (see picture) has been successfully synthesized by a combination of solid- and solution-phase peptide synthesis. Chemically synthesized Lan-A2 (**2**) exhibits synergistic biological activity similar to natural lacticin A2 (**1**) in the presence of natural lacticin A1 against Gram-positive bacteria.

Lantibiotic Synthesis

V. R. Pattabiraman, S. M. K. McKinnie,
J. C. Vederas* ______ **9472 – 9475**

Solid-Supported Synthesis and Biological Evaluation of the Lantibiotic Peptide Bis(desmethyl) Lacticin 3147 A2

Catching the worm: Long myelin-like tubules of a polyethylene oxide-polybutylene oxide block copolymer are kinetically unstable but can be trapped by silica incorporation to produce hybrid nanostructures with high shape anisotropy (see TEM image). Sequestration of mixtures of organosilanes and metal alkoxides or drug molecules in the polymer mesophase gives rise to a range of novel functional nanomaterials.

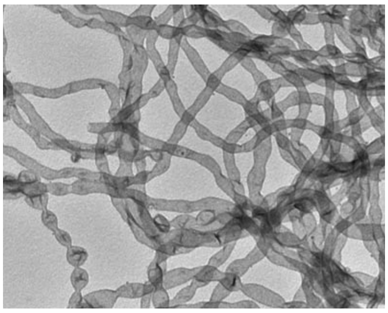

Nanostructures

M. Li, S. Mann* ______ **9476 – 9479**

Emergent Hybrid Nanostructures Based on Non-Equilibrium Block Copolymer Self-Assembly

A magnetic coordination polymer, BBDTA·$InBr_4$, undergoes a spin-Peierls-like phase transition at 250 K. X-ray crystal analysis illustrates that the lattice dimerization accompanies elongation and contraction of the In–N coordination bonds. Inhomogeneity of the spin and charge distribution on the organic radical increases progressively as the temperature decreases below the transition temperature.

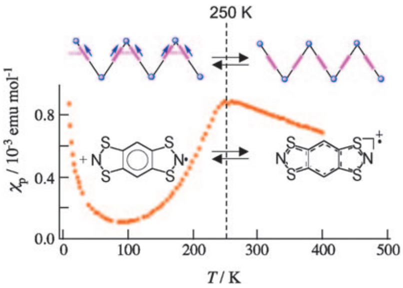

Organic Magnets

W. Fujita,* K. Kikuchi,
K. Awaga ______ **9480 – 9483**

Structural Study of a Dimerization Process in an Organic Radical Magnet, BBDTA·$InBr_4$

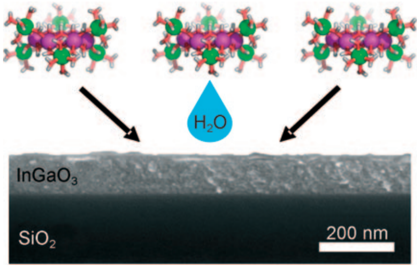

Cluster's last stand: The hydrated gallium/indium nanocluster $[Ga_7In_6(\mu_3\text{-}OH)_6(\mu\text{-}OH)_{18}(H_2O)_{24}(NO_3)_{15}]$ was prepared in a facile, high-yielding synthesis. The use of a key nitroso-containing organic compound as an additive allows for the isolation of multiple grams of the cluster. This larger-scale synthesis facilitates use of the cluster as a single-source precursor for effective thin-film transistors.

Nanoclusters

Z. L. Mensinger, J. T. Gatlin, S. T. Meyers,
L. N. Zakharov, D. A. Keszler,*
D. W. Johnson* ______ **9484 – 9486**

Synthesis of Heterometallic Group 13 Nanoclusters and Inks for Oxide Thin-Film Transistors

Contents

Porous Materials

L.-G. Qiu,* T. Xu, Z.-Q. Li, W. Wang, Y. Wu,
X. Jiang, X.-Y. Tian,
L.-D. Zhang ______ **9487 – 9491**

Hierarchically Micro- and Mesoporous Metal–Organic Frameworks with Tunable Porosity

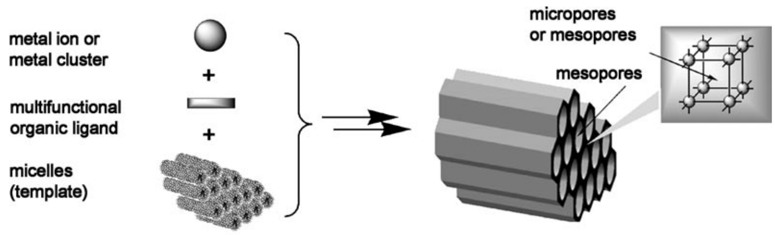

A new hierarchy: A supramolecular template strategy is used to synthesize hierarchical micro- and mesoporous metal–organic frameworks. The mesopore walls are constructed from a microporous framework (see picture). The porosity can be tuned by using different templates at various molar ratios.

Enzyme Models

M. L. Singleton, N. Bhuvanesh,
J. H. Reibenspies,
M. Y. Darensbourg* ______ **9492 – 9495**

Synthetic Support of De Novo Design: Sterically Bulky [FeFe]-Hydrogenase Models

A twisted mimic: Upon oxidation of $[(\mu\text{-}SCH_2C(CH_3)_2CH_2S\text{-})\{Fe^I(CO)_2PMe_3\}_2]$, rearrangement yields the mixed-valent Fe^IFe^{II} cation in a square-pyramid/inverted square-pyramid geometry with a semibridging CO ligand, closely mimicking the [FeFe] hydrogenase enzyme active site. According to de novo design principles, the steric effect of bridgehead bulk in the S–S bridging ligand stabilizes this structure in the absence of the protein matrix.

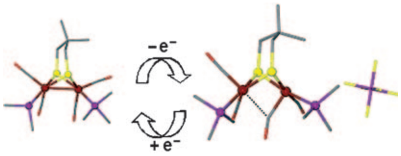

Ultrafast Diffraction

S. T. Park, A. Gahlmann, Y. He,
J. S. Feenstra, A. H. Zewail* **9496 – 9499**

Ultrafast Electron Diffraction Reveals Dark Structures of the Biological Chromophore Indole

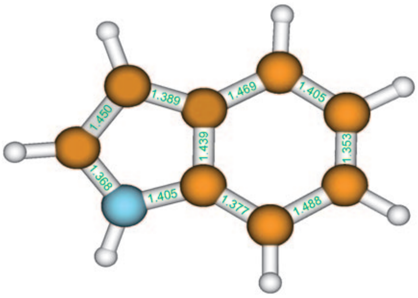

Shedding a light on the dark: Ultrafast electron diffraction of the tryptophan chromophore, indole (see determined structure; C orange, N blue, H white), reveals the involvement of dark structures in the nonradiative pathways of the isolated molecule. Such dark structures have to be part of the understanding of biological chromophore stability.

Near-Infrared Emitter

E. G. Moore, G. Szigethy, J. Xu,
L.-O. Pålsson, A. Beeby,
K. N. Raymond* ______ **9500 – 9503**

3-Hydroxypyridin-2-one Complexes of Near-Infrared (NIR) Emitting Lanthanides: Sensitization of Holmium(III) and Praseodymium(III) in Aqueous Solution

Ho ho ho! Characteristic visible and near-infrared (NIR) emission bands of the Pr^{III} and Ho^{III} complexes of the tetradentate 1-methyl-3-hydroxypyridin-2-one chromophore are observed in aqueous solution. The Ho^{III} complex has been structurally characterized and, for the first time for a Ho^{III} complex, the kinetics of the luminescence decay in the NIR region have been determined in solution.

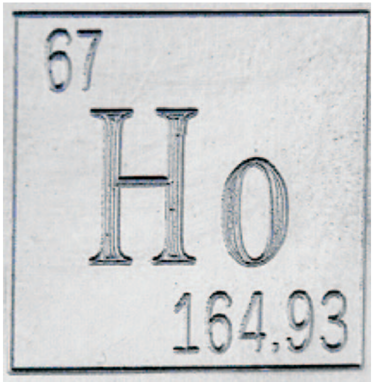

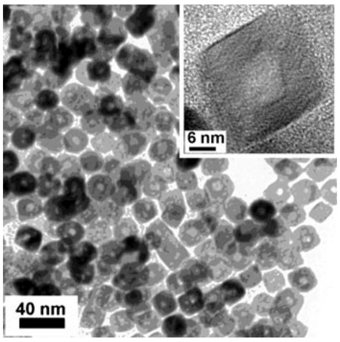

Hollow nan': Hollow face-centered cubic (fcc) Co nanoparallelepipeds were prepared by thermolysis of solid fcc CoO nanoparallelepipeds in oleylamine (see TEM image). The solid fcc CoO nanoparallelepipeds are reduced by the oleylamine surfactant to form hollow fcc Co nanoparallelepipeds. Voids and fcc Co are generated on the surface of the solid fcc CoO nanoparallelepipeds by the removal of oxide as carbon monoxide.

Hollow Nanoparticles

K. M. Nam, J. H. Shim, H. Ki, S.-I. Choi, G. Lee, J. K. Jang, Y. Jo, M.-H. Jung, H. Song,* J. T. Park* ——— **9504 – 9508**

Single-Crystalline Hollow Face-Centered-Cubic Cobalt Nanoparticles from Solid Face-Centered-Cubic Cobalt Oxide Nanoparticles

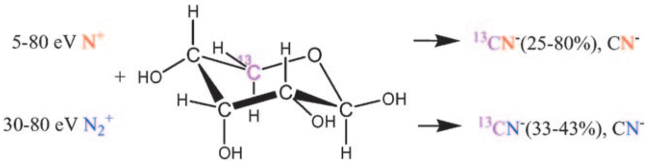

Stealing C: Scattering of hyperthermal nitrogen ions from a D-ribose film efficiently abstracts carbon from the molecule to form CN (see scheme). The reaction is strongly bond and energy selective for C5 of D-ribose in its pyranose form. The sugar moiety of the DNA/RNA backbone will thus be a vulnerable point for damage caused by reactive scattering of secondary atomic nitrogen ions produced by energetic heavy ions.

DNA Damage

VIP

Z. Deng, I. Bald, E. Illenberger, M. A. Huels* ——— **9509 – 9512**

Bond- and Energy-Selective Carbon Abstraction from D-Ribose by Hyperthermal Nitrogen Ions

Pure and porous: Several hundreds of square meters of enantiopure surface per gram of material were generated by introducing amino acids into periodically ordered mesoporous organosilica materials. The stereochemical nature of the surfaces was probed by measuring adsorption isotherms with chiral gases.

Porous Materials

A. Kuschel, H. Sievers, S. Polarz* ——— **9513 – 9517**

Amino Acid Silica Hybrid Materials with Mesoporous Structure and Enantiopure Surfaces

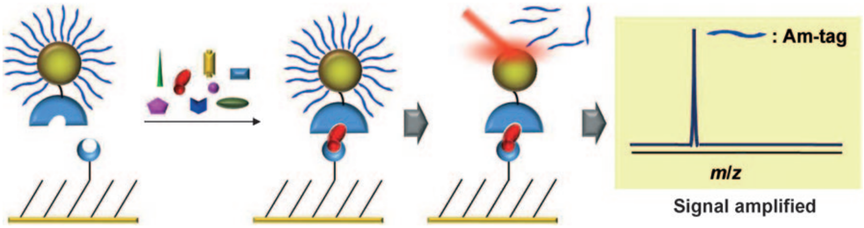

Small but more than enough: Proteins are detected in solution without additional amplification or labeling steps by using a small molecule as a reporter of the protein (see picture, Am-tag = amplification tag). The combination of self-assembled monolayers on gold with matrix-free laser desorption/ionization time-of-flight mass spectrometry offers ultrahigh sensitivity with a detection limit of several attomoles.

Signal Amplification

J. R. Lee, J. Lee, S. K. Kim, K. P. Kim, H. S. Park,* W.-S. Yeo* ——— **9518 – 9521**

Mass Spectrometry Signal Amplification Method for Attomolar Detection of Antigens Using Small-Molecule-Tagged Gold Microparticles

Luminescence Switching

T. Mutai,* H. Tomoda, T. Ohkawa, Y. Yabe, K. Araki* ———— 9522 – 9524

Switching of Polymorph-Dependent ESIPT Luminescence of an Imidazo[1,2-*a*]pyridine Derivative

Reproducible switching of the polymorph-dependent excited-state intramolecular proton-transfer (ESIPT) luminescence of an imidazo[1,2-*a*]pyridine between blue-green and yellow (see picture) is achieved by thermal control of its solid-state molecular packing. Thus, ESIPT is a promising mechanism for packing-to-luminescence transduction and amplification that offers a novel design concept for tunable organic luminescent solids.

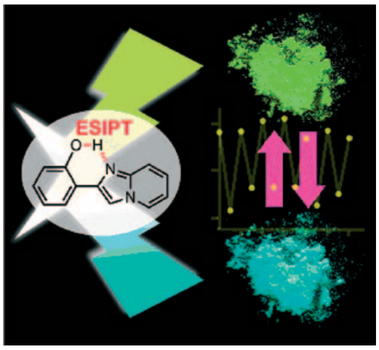

Two-Photon Photolysis

S. Gug, F. Bolze,* A. Specht, C. Bourgogne, M. Goeldner, J.-F. Nicoud ———— 9525 – 9529

Molecular Engineering of Photoremovable Protecting Groups for Two-Photon Uncaging

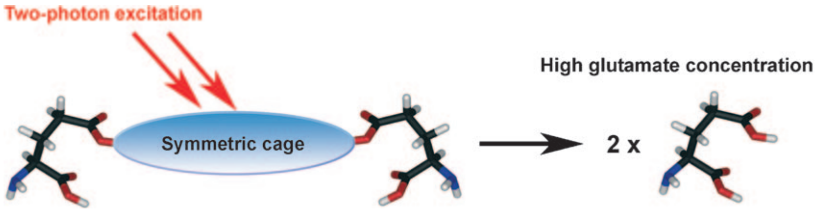

Open the cage: Symmetrical photoremovable bis-glutamate cages have been designed, synthesized, and characterized that can release a neurotransmitter with unprecedented two-photon efficiencies (see picture), up to 5 GM for BNSF–Glu (BNSF = 2,7-bis-{4-nitro-8-[3-(2-propyl)-styryl]}-9,9-bis-[1-(3,6-dioxaheptyl)]-fluorene) at 800 nm, the optimal window both for tissue transparency and classically available laser sources.

Bismuth–Nitrogen Cations

W. Baumann, A. Schulz,* A. Villinger ———— 9530 – 9532

A Blue Homoleptic Bismuth–Nitrogen Cation

Bi and N form a W: An acyclic Bi–N cation (synthesized as its GaCl_4^- salt) was prepared from lithium *N*,*N*′,*N*′-tris(trimethylsilyl)hydrazide and BiCl_3 by chloride abstraction. The W-shaped NNBiNN structure and the bonding of this deep blue cation, which can be regarded a bismapentazenium cation, is discussed on the basis of experimental and theoretical data.

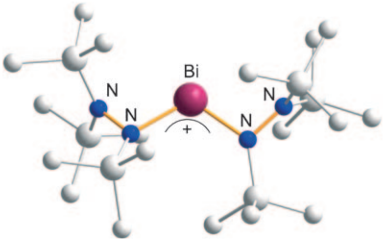

Enzymatic Halogenation

S. Flecks, E. P. Patallo, X. Zhu, A. J. Ernyei, G. Seifert, A. Schneider, C. Dong, J. H. Naismith, K.-H. van Pée* ———— 9533 – 9536

New Insights into the Mechanism of Enzymatic Chlorination of Tryptophan

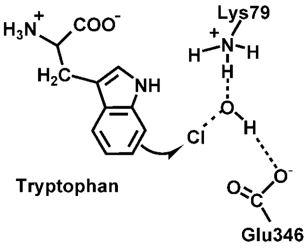

It takes two: Both a lysine and a glutamate residue in the active site of tryptophan halogenase are essential for its chlorination activity. A mechanism for the regioselective enzymatic chlorination of tryptophan involving both amino acids is suggested (see scheme).

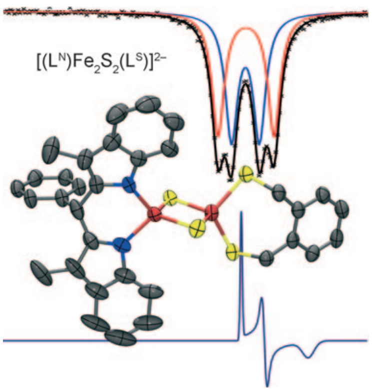

Copycat: An accurate synthetic model for Rieske type [2Fe-2S] cluster has been prepared that emulates structural and spectroscopic features of the natural protein sites, including the characteristic low g_{av} value in the EPR spectra of the reduced [2Fe-2S]$^+$ species. The picture shows the crystal structure of the molecule (C gray, Fe red, N blue, S yellow), its EPR spectrum after reduction (bottom) and its Mössbauer spectrum (top).

Bioinorganic Chemistry

J. Ballmann, A. Albers, S. Demeshko, S. Dechert, E. Bill, E. Bothe, U. Ryde, F. Meyer* ______ **9537 – 9541**

A Synthetic Analogue of Rieske-Type [2Fe-2S] Clusters

Not like the others: A molecular palladium oxide cluster was formed by self-assembly of palladium(II) and arsenic(V) using mild reaction conditions. The resulting heteropolypalladate $[Pd^{II}_{13}As^{V}_{8}O_{34}(OH)_6]^{8-}$ has a distorted cubic shape and edge lengths of about 1 nm. The thirteen Pd^{II} ions retain four-coordinate square-planar geometry, in marked contrast to all other known discrete polyoxometalates.

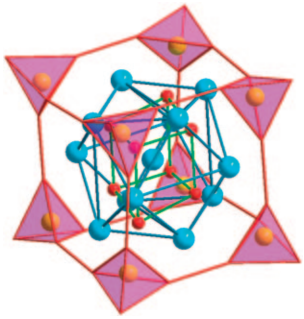

Polyoxometalates

E. V. Chubarova, M. H. Dickman, B. Keita, L. Nadjo, F. Miserque, M. Mifsud, I. W. C. E. Arends, U. Kortz* **9542 – 9546**

Self-Assembly of a Heteropolyoxopalladate Nanocube: $[Pd^{II}_{13}As^{V}_{8}O_{34}(OH)_6]^{8-}$

Without a transition metal, unsaturated organomagnesium compounds undergo homocoupling in the presence of a substoichiometric amount of the oxidant 2,2,6,6-tetramethylpiperidine-*N*-oxyl radical (TEMPO) and oxygen. Alkynyl Grignard reagents can even be coupled to give the corresponding diynes with dioxygen in the absence of a catalyst (see scheme).

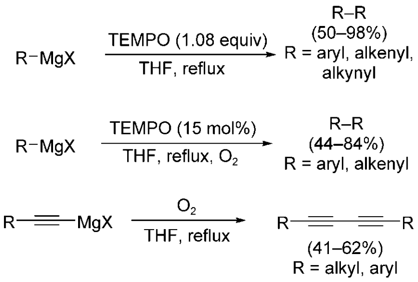

Synthetic Methods

M. S. Maji, T. Pfeifer, A. Studer* ______ **9547 – 9550**

Oxidative Homocoupling of Aryl, Alkenyl, and Alkynyl Grignard Reagents with TEMPO and Dioxygen

---

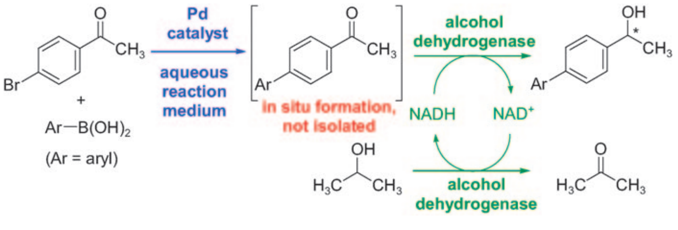

Two breeds of cat: A palladium-catalyzed Suzuki cross-coupling and an enzymatic reduction with an alcohol dehydrogenase from *Rhodococcus* sp. together enable the efficient and highly enantioselective synthesis of chiral biaryl alcohols in a one-pot process (see scheme).

Aqueous Catalysis

E. Burda, W. Hummel, H. Gröger* ______ **9551 – 9554**

Modular Chemoenzymatic One-Pot Syntheses in Aqueous Media: Combination of a Palladium-Catalyzed Cross-Coupling with an Asymmetric Biotransformation

Molecular Beacons

E. Socher, L. Bethge, A. Knoll, N. Jungnick, A. Herrmann, O. Seitz* ____ **9555 – 9559**

Low-Noise Stemless PNA Beacons for Sensitive DNA and RNA Detection

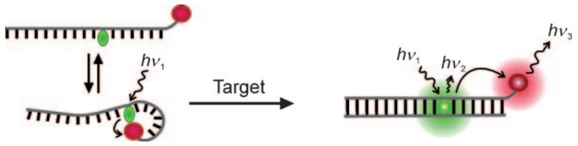

A change of the energy transfer mechanism (from contact quenching to FRET) increases the responsiveness of fluorescent hybridization probes. The communication between a responsive fluorescent base surrogate (see picture, green) and a near-infrared dye (red) in peptide nucleic acid provides probes that are extremely dark in the single strand. Hybridization furnishes strong fluorescence increase with a 200 nm shift in emission maximum.

Rare-Earth Metal Complexes

R. Litlabø, M. Zimmermann, K. Saliu, J. Takats, K. W. Törnroos, R. Anwander* ____________ **9560 – 9564**

A Rare-Earth Metal Variant of the Tebbe Reagent

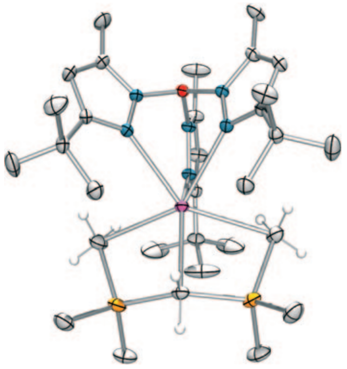

The Trofimenko–Tebbe alliance: The sterically crowded, monoanionic scorpionate ligand $\mathrm{Tp}^{t\mathrm{Bu,Me}}$ provides a unique environment for the isolation of discrete rare-earth metal complexes with $\mathrm{Y{-}(CH_3)\{Al(CH_3)_4\}}$ and $\mathrm{La{-}(CH_2)}$ moieties (see structure; C gray, H white, Al orange, B red, La pink, N blue); the latter shows promising reactivity as a Tebbe reagent analogue.

Photoaffinity Labeling

X. Bi, A. Schmitz, A. M. Hayallah, J.-N. Song, M. Famulok* ___ **9565 – 9568**

Affinity-Based Labeling of Cytohesins with a Bifunctional SecinH3 Photoaffinity Probe

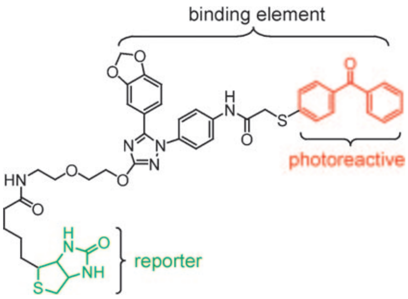

The specific binding of the cytohesin inhibitor SecinH3 to Sec7 domains of cytohesins was shown by the use of a bifunctional photoaffinity probe (see structure) on guanine nucleotide exchange factors (GEFs) and GTPases. This probe should be useful for the proteome-wide profiling of cytohesin complexes and the identification of the binding site.

Supporting information is available on www.angewandte.org (see article for access details).

A video clip is available as Supporting Information on www.angewandte.org (see article for access details).

Service

Spotlights Angewandte's Sister Journals ____ *9376*
Keywords ____ *9570*
Authors ____ *9571*
Vacancies ____ *9373, 9379*
Preview ____ *9573*